B lymphocytes trigger monocyte mobilization and impair heart function after acute myocardial infarction

Yasmine Zouggari[1,12], Hafid Ait-Oufella[1,2,12], Philippe Bonnin[3], Tabassome Simon[2,4], Andrew P Sage[5], Coralie Guérin[1], José Vilar[1], Giuseppina Caligiuri[6], Dimitrios Tsiantoulas[7,10], Ludivine Laurans[1], Edouard Dumeau[1], Salma Kotti[4], Patrick Bruneval[1,8], Israel F. Charo[9], Christoph J. Binder[7,10], Nicolas Danchin[8] , Alain Tedgui[1], Thomas F. Tedder[11], Jean-Sébastien Silvestre[1,12], Ziad Mallat[1,5,12]

[1]Institut National de la Santé et de la Recherche Médicale (Inserm), Unit 970, Paris Cardiovascular Research Center, and Université Paris-Descartes, Paris, France.

[2]Assistance Publique, Hôpitaux de Paris, Université Pierre et Marie Curie, Paris, France.

[3] Université Paris-Diderot, Sorbonne Paris Cité, INSERM, UMR-S 965, AP-HP, Hôpital Lariboisière, Paris, France.

[4]URC-EST, Hôpital Saint Antoine Paris, France.

[5]Division of Cardiovascular Medicine, University of Cambridge, Addenbrooke's Hospital, Cambridge, CB2 2QQ, UK.

[6]Inserm, Unit 698, Paris, France.

[7]Center for Molecular Medicine, Austrian Academy of Sciences, Vienna, Austria.

[8]Assistance Publique, Hôpitaux de Paris, Université Paris-Descartes, Paris, France.

[9]Gladstone Institute of Cardiovascular Disease, San Francisco, California, USA.

[10]Department of Laboratory Medicine, Medical University of Vienna, Austria.

[11]Department of Immunology, Duke University Medical Center, Durham, North Carolina, USA.

[12]These authors contributed equally to this work.

Correspondence should be addressed to: Ziad Mallat, MD, PhD, at Division of Cardiovascular Medicine, University of Cambridge, Addenbrooke's Hospital, Cambridge, CB2 2QQ, UK. E-Mail: zm255@medchl.cam.ac.uk.

Abstract

Acute myocardial infarction (MI) is a severe ischemic disease responsible for heart failure and sudden death. Here, we show that following acute MI in mice, mature B lymphocytes selectively produce Ccl7 and induce Ly6C^{hi} monocyte mobilization and recruitment, leading to enhanced tissue injury and deterioration of myocardial function. Genetic (*Baff-r* deficiency) or antibody-mediated (CD20- or Baff-specific antibody) depletion of mature B lymphocytes impedes Ccl7 production and monocyte mobilization, limits myocardial injury and improves heart function. These effects are recapitulated in mice with B cell selective *Ccl7* deficiency. We also show that elevated circulating levels of Ccl7 and Baff in patients with acute MI predict increased risk of death or recurrent MI at follow-up. The work unravels a previously unsuspected interaction between mature B lymphocytes and monocytes following acute ischemia, and identifies novel therapeutic targets for this devastating condition.

Acute thrombotic obstruction of the blood flow in coronary arteries precipitates myocardial infarction (MI) with deleterious consequences on heart function [1-4]. The mainstay of treatment involves rapid restoration of a patent coronary artery either mechanically or through thrombolytic and anti-platelet therapies, and administration of agents that reduce oxygen consumption and unload the heart muscle [1,5]. Still, the clinical and social burden of ischemic heart disease is unacceptably high and the efficacy of additional anti-thrombotic therapies is often mitigated by the increased risk of hemorrhagic events. Thus, efforts are being directed towards targeting other pathophysiological pathways, particularly those involved in post-ischemic cardiac remodeling [4,6].

The immune system becomes activated in response to myocardial damage [7]. Shortly after ischemia, the damaged tissue exposes ligands (i.e., non-myosin heavy chain type IIA and C) that are recognized by components of the innate immune system, which leads to its activation [8-12]. C-reactive protein (CRP), a short pentraxin acute-phase protein, also binds to damaged tissue and activates complement, leading to aggravation of tissue injury in the setting of acute MI [13]. In contrast, long pentraxin 3, a molecule that limits complement activation plays a cardioprotective role in this setting [14]. The acute inflammatory response also leads to the mobilization and recruitment of innate immune cells. Few hours after the ischemic insult, neutrophils are actively recruited into the ischemic tissue and contribute to tissue inflammation and cardiovascular injury through the production of inflammatory mediators, reactive oxygen species and various proteases [15,16]. The wave of neutrophil infiltration is followed by the mobilization and recruitment of monocytes. Recent studies

have shed new light on the mechanisms of monocytes recruitment and life cycle in the setting of acute MI. The studies suggested differential pathogenic or protective roles for $Ly6C^{hi}$ and $Ly6C^{lo}$ monocytes, respectively, in cardiac remodeling and preservation of heart function [17,18]. Despite this increasing knowledge, the utility of targeting the immune response in this setting is still uncertain as revealed by the lack of efficacy of complement inhibition in patients with acute MI [19-22]. Thus, a better characterization of the determinants of the immune response following ischemic injury and the mechanisms by which they contribute to tissue damage is required in order to fill the existing gap of knowledge that limits clinical translation, and design efficient therapeutic strategies for future use in humans.

Here, we addressed the role of mature B lymphocytes, a subset of immune cells that orchestrates a variety of adaptive immune responses relevant to human diseases [23], but that has relatively been neglected in the setting of ischemic injury. We show that following acute MI in mice, mature B lymphocytes are activated to produce Ccl7, a chemokine that induces monocyte mobilization from the bone marrow, leading to enhanced myocardial inflammation, tissue injury and deterioration of myocardial function.

RESULTS

Mature B cells are recruited to the ischemic tissue after MI

To identify the inflammatory cell repertoire within the injured myocardium, we induced acute MI in C57BL/6J mice by permanent coronary artery ligation and analyzed cell suspensions of digested infarcts at different time points by flow cytometry. We found that

neutrophils ($CD11b^+$ $Ly6G^{hi}$ $7/4^{hi}$ cells) peaked as early as day 1 after MI **(Supplementary Fig. 1a)**, followed by successive waves of $7/4^{hi}$ ($Ly6C^{hi}$) and $7/4^{lo}$ ($Ly6C^{lo}$) monocytes ($CD11b^{hi}$ $Ly6G^-$) **(Supplementary Fig. 1b),** and by accumulation of dendritic cells, macrophages and Natural Killer cells **(Supplementary Fig. 1c and 1d)**. We also found that $CD3^+$ T lymphocytes accumulated in the injured myocardium within 1 day after MI and dropped thereafter **(Supplementary Fig. 1e).** The results are in agreement with previous studies [17]. Intriguingly, the duration and the intensity of B lymphocyte infiltration into the ischemic cardiac tissue remain largely undefined. We found that B lymphocytes, defined as $B220^+$ IgM^+ cells, accumulated in the infarct area, peaked on day 5 after MI and waned thereafter to levels comparable to those in sham-operated mice **(Supplementary Fig. 2a)**. Immunohistological and additional flow cytometry analyses confirmed the increased accumulation of B220-positive and $CD19^+IgD^+IgM^{low}$ B lymphocytes in the border infarct area after MI compared to sham-operated animals **(Supplementary Fig. 2b and 2c)**. Thus, myocardial infarction triggers the infiltration of circulating mature B lymphocytes into cardiac tissue, suggesting a potential role of B cell-mediated immune response in this setting.

B cell depletion prevents adverse remodeling and improves cardiac function

To directly assess the role of mature B lymphocytes in cardiac remodeling after MI, we depleted B lymphocytes using a CD20-specific monoclonal antibody (CD20 mAb) [24,25]. As expected, we found that CD20 mAb treatment led to sustained and profound reduction of the number of mature B lymphocytes in cardiac tissue (**Supplementary Fig. 3a)**, the peripheral blood **(Fig. 1a)** and the spleen **(Supplementary Fig. 3b)**. Both follicular (FO)

and marginal zone (MZ) B cells were depleted (**Supplementary Fig. 3c)** whereas B1 cells were preserved during the duration of the experiment (data not shown)[26]. We next assessed cardiac function by echocardiography 14 days after MI. Of interest, CD20 mAb-induced B cell depletion led to a reduction in end-systolic left ventricular (LV) dimension ($P = 0.016$), a significant improvement of LV shortening fraction ($P = 0.021$) and an increase in LV myocardial contractility ($P = 0.025$) compared to control animals **(Fig. 1b)**. This was associated with a reduction of infarct size ($P = 0.024$) and interstitial fibrosis as assessed by collagen content ($P = 0.016$) **(Fig. 1c)**. In addition, B cell depletion reduced the number of apoptotic cells within the injured myocardium, as shown by TUNEL staining ($P = 0.005$) but had no effect on neovascularization **(Supplementary Fig. 4)**. Overall, these results show that systemic B cell depletion significantly reduces post-ischemic injury, prevents adverse ventricular remodeling and improves cardiac function after acute MI.

B cell depletion reduces both systemic and local pro-inflammatory responses

We next assessed the potential mechanisms involved in B cell-mediated effects on cardiac remodeling and function. Previous studies reported a pathogenic role for natural IgM antibodies in the first 24 hours following ischemia-reperfusion injury [11,27]. We therefore assessed changes in antibody production after CD20 mAb treatment. Mature B cell depletion did not alter IgM or IgG levels in the first three days after MI, making unlikely the hypothesis of an antibody-mediated effect (**Supplementary Fig. 5**). The moderate decrease of IgM levels at day 14 after MI in CD20 mAb-treated animals (**Supplementary Fig. 5**) might be secondary to the reduction of myocardial necrosis.

We next assessed changes in the inflammatory response. Treatment with CD20 mAb resulted in a profound reduction of both systemic and local pro-inflammatory cytokines measured at day 14 after MI. Hence, IL-1β ($P = 0.04$), TNF-α ($P = 0.004$) and IL-18 ($P = 0.041$) mRNA levels were significantly lower in infarct hearts of B cell depleted-mice compared to the control group **(Fig. 1d)**. In contrast, expression of anti-inflammatory mediators, IL-10 and TGF-β, tended to be unaffected in the B cell-depleted animals **(Fig. 1d)**. Similar results were found in spleens and lymph nodes of B cell-depleted mice **(Supplementary Fig. 6a and 6b)**, suggesting a limited inflammatory response.

B cell depletion impairs monocyte mobilization and recruitment after acute MI

We then addressed the mechanisms that could account for the reduced inflammatory response and the improvement in ventricular remodeling. A striking observation was that B cell-depleted mice constantly showed altered monocyte compartmentalization as revealed by enhanced accumulation of $7/4^{hi}$ monocytes in the bone marrow ($P = 0.01$ vs controls) **(Fig. 2a)** and the spleen (p=0.02 vs controls) (**Supplementary Fig. 7)**, associated with a significant decrease of their circulating blood count ($P = 0.015$ vs PBS) **(Fig. 2b)**, suggesting impaired monocyte mobilization.

We also addressed the effect of CD20-mediated B cell depletion on monocyte recruitment from the circulating blood into the ischemic heart. Mice underwent coronary artery ligation and were treated (1h after ligation) with either PBS or CD20 mAb. Four hours after MI, the 2 groups of mice received an intravenous infusion of $CD45.1^+$ mononuclear cells (15×10^6). We then quantified the number of recruited $CD45.1^+$ $CD11b^+ Ly6G^- Ly6C^+$ cells in the myocardium 3 days after monocyte transfer. As shown

in **Fig. 2c**, CD20-mediated B cell depletion led to substantial reduction in monocyte recruitment into the ischemic myocardium. We also found a non-significant trend towards reduced accumulation of $7/4^{hi}$ monocytes (**Supplementary Fig. 8a**) and a substantial reduction of macrophage accumulation within the ischemic heart 3 and 5 days after CD20 mAb treatment, respectively (**Fig. 2d**). Other cell subsets were not altered (**Supplementary Fig. 8b and 8c**).

B lymphocytes produce Ccl7 and trigger monocyte migration

Since Ccr2-mediated signals are required for monocyte mobilization from the bone marrow [17,28] and recruitment into injured tissues, we examined potential changes in the production of Ccl2 and Ccl7, the 2 major Ccr2 ligands. We found that acute MI led to a significant increase of both Ccl2 and Ccl7 mRNA and protein levels, in blood and cardiac tissue (**Supplementary Fig. 9)**. Intriguingly, B cell depletion was associated with a significant and selective impairment of Ccl7 levels ($P = 0.03$) compared to the control group, while Ccl2 (and Ccl12) levels were not significantly affected by B cell depletion **(Fig. 3a and Supplementary Fig. 9)**.

These results suggested that B lymphocytes might produce Ccl7 and induce Ccl7-dependent monocyte mobilization. To address this hypothesis, we first evaluated Ccl7 expression by splenic B cells using flow cytometry and RT-qPCR. We found that $CD19^{+}$ B lymphocytes, which are markedly depleted after CD20 mAb treatment, express Ccl7, with higher expression after myocardial infarction (**Supplementary Fig. 10**). Interestingly, spleen B cells of *Myd88*$^{-/-}$*Trif*$^{-/-}$ mice produced substantially less Ccl7 than B cells of WT animals after MI (**Supplementary Fig. 10**). We also assessed Ccl7

secretion by cultured B lymphocytes. Whereas Ccl2 and Ccl12 remained undetectable in supernatants of B lymphocytes (data not shown), these cells produced significant amount of Ccl7, which was further increased after their activation with anti-CD40 and anti-IgM antibodies (data not shown) or with TLR agonists, particularly CpG (**Fig. 3b and Supplementary Fig. 10**). We also found that activated cultured B lymphocytes strongly enhanced 7/4^{hi} monocytes transmigration *in vitro* compared to non-stimulated B lymphocytes ($P < 0.0001$) **(Fig. 3c)**. Interestingly, neutralizing anti-Ccl7 antibody abrogated B cell-induced migration of cultured 7/4^{hi} monocytes ($P = 0.0003$), while Ccl2 neutralization had no effects (**Fig. 3c**).

Ccl7-deficient B cells fail to affect cardiac remodeling and function after acute MI

These findings prompted us to investigate the direct role of B cell-derived Ccl7 in post-ischemic cardiac remodeling. First, we unraveled a key role of Ccl7 in this setting using Ccl7-deficient mice. We found that following acute MI, Ccl7 deficiency was associated with a reduction of 7/4^{hi} monocyte mobilization from bone marrow ($P = 0.013$ vs WT) to the blood ($P = 0.04$ vs WT), and improvement of cardiac function **(Supplementary Fig. 11)**. To further substantiate the role of B cell-derived Ccl7 in this setting, we injected *Rag1*$^{-/-}$ mice either with wild-type splenocytes, B cell-depleted splenocytes, or B cell-depleted splenocytes re-supplemented with wild-type or *Ccl7*$^{-/-}$ B lymphocytes. The purity of the B lymphocytes is shown in **Supplementary Fig. 12**. We first verified that re-supplementation with wild-type or *Ccl7*$^{-/-}$ B lymphocytes significantly increased B cell numbers in spleens of *Rag1*$^{-/-}$ mice compared to mice injected with B cell-depleted splenocytes only **(Supplementary Fig. 12)**. We then evaluated circulating Ccl7 levels

and found that re-supplementation with wild-type B lymphocytes was associated with an increase of Ccl7 levels compared to mice receiving B cell-depleted splenocytes only (968.5 ± 46.06 pg ml^{-1} and 201.1 ± 28.31 pg ml^{-1}, respectively, $P < 0.0001$). In contrast, re-supplementation of B cell-depleted splenocytes with B lymphocytes isolated from *Ccl7*$^{-/-}$ mice failed to increase Ccl7 levels (152.6 ± 39.9 pg ml^{-1}, $P < 0.0001$ vs wild-type B lymphocytes). Interestingly, we also found that re-supplementation with wild-type B lymphocytes was associated with an increase of 7/4^{hi} monocyte numbers in the blood and within the injured myocardium compared to the group receiving B cell-depleted splenocytes only **(Fig. 3d)**, a phenotype that was abrogated in mice re-supplemented with *Ccl7*$^{-/-}$ B lymphocytes **(Fig. 3d)**. Thus, B cell-derived Ccl7 triggers selective mobilization and tissue recruitment of 7/4^{hi} monocytes after acute MI.

We then examined the consequences of Ccl7 deficiency in B lymphocytes on post-ischemic cardiac remodeling. We found that transfer of B cell-depleted splenocytes into *Rag1*$^{-/-}$ mice reduced end-systolic LV chamber dimension ($P = 0.04$) and improved left ventricular shortening fraction ($P = 0.008$) after MI compared to the transfer of non-depleted splenocytes **(Fig. 4a)**. This effect was abrogated after re-supplementation of B cell-depleted splenocytes with B lymphocytes isolated from wild-type mice ($P = 0.0007$ and $P = 0.02$ respectively) but was not altered after re-supplementation with *Ccl7*$^{-/-}$ B lymphocytes **(Fig. 4a)**. B cell depletion also reduced infarct size (p=0.04; **Fig. 4b**) and collagen content (**Fig. 4c**), which was antagonized by re-supplementation with wild-type but not with *Ccl7*$^{-/-}$ B lymphocytes **(Fig. 4b and 4c)**. Circulating IgM and IgG levels were similar in mice re-supplemented with wild-type versus *Ccl7*$^{-/-}$ B lymphocytes (**Supplementary Fig. 12**), making unlikely a contribution of humoral immunity to the

cardioprotective effect, although we did not measure specific antibody titers.

We also generated a B cell-restricted Ccl7 deficient mouse model by reconstituting lethally-irradiated wild-type animals with a mixture of bone marrow from *μMT* and *Ccl7*$^{-/-}$ mice (see Methods online). The control group received a mixture of *μMT* and *Ccl7*$^{+/+}$ bone marrow. Again, we found that restricted Ccl7 deficiency in B lymphocytes led to reduction of circulating Ccl7 levels (**Fig. 4d**) and improved heart function after acute MI (**Fig. 4e**).

Blockade of Baff signaling impairs monocyte mobilization and improves heart function

Baff signaling through Baff receptor (Baff-r) is required for the maintenance of mature B2 cells and *Baff-r*$^{-/-}$ mice are characterized by a profound reduction of follicular (FO) and marginal zone (MZ) B lymphocytes but preservation of B1 cells [29] (and **Supplementary Fig. 13**). We therefore addressed the impact of *Baff-r* deficiency on the pathophysiology of post-ischemic myocardial injury. Interestingly, we found that *Baff-r*$^{-/-}$ mice showed a significant increase in the accumulation of Ly6C^{hi} monocytes in the bone marrow but displayed lower levels of these monocytes in the circulating blood compared with control littermates (**Fig. 5a and Supplementary Fig. 13**), clearly suggesting impaired monocytes mobilization. This was associated with reduced levels of circulating Ccl7 in *Baff-r*$^{-/-}$ mice (**Fig. 5b**). Importantly, *Baff-r* deficiency improved heart function after MI as shown by the significant increase of shortening fraction in *Baff-r*$^{-/-}$ mice compared with *Baff-r*$^{+/-}$ littermates (**Fig. 5c**) despite no change in infract size (**Supplementary Fig. 13**). To further substantiate the role of Baff in this context, we

treated a group of wild-type mice with anti-Baff monoclonal antibody (see Methods online). We found that Baff neutralization led to significant depletion of circulating B lymphocytes (**Fig. 5d**), which was associated with impaired Ly6C^{hi} monocyte mobilization (**Fig. 5e and Supplementary Fig. 13)** and improved cardiac function (**Fig. 5f**).

Circulating levels of CCL7 and BAFF predict adverse cardiovascular outcome

Finally, we addressed the relevance of these findings to the human disease by assessing the relationship between circulating CCL7 or BAFF levels and clinical outcomes in a cohort of 1,000 patients admitted for acute MI. Patients' characteristics are given in **Supplementary Table 1 and Supplementary Table 2**. Interestingly, we found that patients with detectable circulating levels of CCL7 at their admission for acute MI were at substantially increased risk of death and recurrent myocardial infarction after two years of follow-up compared to patients with no detectable CCL7 levels even after adjustment for several multivariable risk factors (see Methods) (hazard ratio, HR=1.54, 95% CI = 1.07-2.43, $P = 0.02$) (**Fig. 6a**). Similarly, the risk of death and recurrent MI was associated with increasing tertiles of circulating BAFF at admission. The HR of death and recurrent MI in the second and third tertiles of BAFF were 1.65 (1.05-2.58) and 3.14 (2.09-4.73) compared with the lowest tertile ($P < 0.0001$). The association remained significant in a fully adjusted model (**Fig. 6b**).

DISCUSSION

B lymphocytes play critical non-redundant roles mediating both innate and adaptive immune responses through antibody-dependent or independent mechanisms. More recent studies identified novel roles for B lymphocytes in the early innate immune response during acute infection [30,31] where B lymphocytes were required to mount an efficient and protective inflammatory response. However, the contribution of B lymphocytes to the inflammatory response secondary to other forms of acute injury, particularly post-ischemic injury is still poorly defined. Our results unravel a critical role for B cell-dependent Ccl7 production in the pathogenic response to acute ischemic injury. The precise B cell subset involved in this setting remains to be examined in more detail. However, our results indicate that it depends in part on Baff-r signaling.

From previous studies, B cell responses appeared to be redundant in post-ischemic stroke injury as B cell-deficient (μMT) mice showed no difference in infarct size or neurological deficit when compared with wild type mice [32]. Other studies addressed the role of B lymphocytes in response to ischemia/reperfusion injury in the kidney. However, the use of B cell-deficient μMT mice by various groups in this setting has led to very divergent results, with studies showing either protection [33,34] or aggravation [12] of ischemia/reperfusion injury in mice lacking B cells. The use of μMT mice should be interpreted with caution given the wide range of associated immune abnormalities and the fact that both innate and adaptive B lymphocytes, with potentially divergent functions, are absent in this strain. A previous study showed that intra-myocardial injection of bone marrow-derived B cells after acute MI in rats improved the recovery of myocardial function [35]. However, there are major differences with the present work. In the previous

study, bone marrow-derived B lymphocytes were mostly immature B cells that are resistant to CD20 mAb-mediated B cell depletion. In addition, the mechanisms of protection afforded by the injection of exogenous immature B lymphocytes remained obscure and the investigators did not assess the role of endogenous B lymphocytes in this setting.

We and others have shown that *Baff-r* deficiency or CD20 mAb-induced B cell depletion holds promise in the context of cardiovascular disease and reduces the development of atherosclerotic lesions in several experimental models [25,36-38]. Our present data clearly show that depletion of mature B lymphocytes after CD20 mAb injection at the acute phase of myocardial infarction leads to significant improvement in both post-ischemic ventricular remodeling and myocardial function. Similar results were obtained using *Baff-r*$^{-/-}$ mice or a neutralizing Baff-specific antibody, although effects on infarct size differed between CD20 mAb treatment and blockade of Baff signaling. It should be noted that Baff receptor is also expressed on non B cells and that B cell depletion was delayed in mice treated with Baff-specific, requiring a second antibody injection at day 1 to obtain a substantial depletion whereas B cells already disappeared from the blood in CD20 mAb-treated mice a few hours after a single injection (**Fig. 1** and data not shown). Future work should address the mechanisms responsible for B cell activation after acute ischemic injury and the pathways that drive B cell-dependent Ccl7 production. For example, several endogenous toll-like receptor ligands may accumulate after necrosis and could lead to B cell activation. In this regard, it is interesting to note that spleen B cells of *Myd88*$^{-/-}$/*Trif*$^{-/-}$ mice produce substantially less Ccl7 than B cells of WT animals. Whether this is related to selective Myd88/Trif signaling in B cells and whether it can

directly impact systemic Ccl7 levels remains to be determined. Moreover, it will be important to address in more detail the contribution of the various B cell and monocyte subsets to post-ischemic injury. The substantial reduction of $Ly6C^{lo}$ monocytes in blood after B cell depletion or blockade of Baff signaling might be in part related to reduced Ccl7 signaling [28] (**Supplementary Fig. 11**) or may suggest the involvement of additional chemokine pathways, like Cx3cr1. However, we found no difference in Cx3cl1 production between CD20-depleted and control animals (data not shown). Finally, pilot data suggest that Cxcl13 may be induced after MI (data not shown) and might play a role in B cell recruitment into the ischemic heart. However, the selective role of B cells that accumulate in the heart after MI is still poorly understood.

In summary, these studies delineate an important contributory role for systemic B cells during the immune responses that lead to tissue damage following acute MI. Neutrophils, monocyte subsets, NK cells and T cells enter the site of injury. The release of inflammatory mediators and tissue antigens appears to result in the rapid activation of B cells systemically leading to B cell production of Ccl7, in part through a MyD88-dependent pathway. B cells are also secondary recruited to the ischemic heart as a component of the inflammatory response. B cell-derived Ccl7 probably synergizes with Ccl7 produced from other cellular sources to increase serum chemokine levels, which facilitates the mobilization of monocytes from the bone marrow and results in enhanced monocyte entry into sites of tissue damage. B cell depletion reduces Ccl7 production and the magnitude of $7/4^{hi}$ monocyte recruitment and macrophage accumulation into post-ischemic tissues. Because B cells are well known to promote pro-inflammatory innate and adaptive immune responses [39], their systemic depletion is likely to further reduce T

cell-, macrophage- and neutrophil-induced tissue damage by reducing the systemic amplification of the inflammatory response following a MI. As a consequence, B cell depletion is shown here to have a profound impact on post-ischemic injury. It substantially limits myocardial inflammation, reduces infarct size and improves myocardial function. The positive associations of BAFF or CCL7 circulating levels with adverse outcomes in patients with acute MI strongly support a clinical relevance to the human disease.

Of note, the depleting CD20 mAb and anti-Baff mAb were administered 1 hour after the induction of myocardial infarction, which mimics clinical settings where a therapeutic agent is administered in the first hours after the onset of clinical symptoms/signs of acute ischemic injury. Thus, we believe that the present study sets the stage for the testing of available humanized B cell-depleting antibodies at the acute phase of myocardial infarction with the aim to limit myocardial necrosis, inflammation and improve the recovery of heart function. In addition, we anticipate that therapies targeting pathways that control mature B lymphocytes, i.e., Baff or Ccl7 pathways, should be of interest in the setting of acute ischemic injury.

ACKNOWLEDGEMENTS

This work was supported by Inserm, British Heart Foundation (Z.M.), European Research Council (Z.M.), Fondation Coeur et Recherche (Z.M., T.S., N.D.), Fondation pour la Recherche Medicale (J.S.S.), European Union Seven Framework programme TOLERAGE (Z.M.), Fondation Leducq transatlantic network (C.J.B., D.T., A.T., J.S.S., Z.M.), National Institutes of Health grants AI56363 and AI057157, and a grant from The Lymphoma Research Foundation (T.F.T). We are indebted to Maria Ozsvar Kozma, Lauren Baker and James Harrison for excellent technical assistance. The anti-Baff antibody was a kind gift from Human Genome Sciences Inc, USA. Y.Z. is a recipient of fellowships from Fondation pour la Recherche Médicale and from Journées de Biologie Clinique. We thank the physicians who cared for the patients at the participating institutions, the International Clinical Trials Association Contract Research Organization (Fontaine-lès-Dijon, France), Elodie Drouet and the Clinical Research Assistant team of Unité de Recherche Clinique de l'Est Parisien (Assistance Publique–Hôpitaux de Paris and UPMC Paris 06), Benoît Pace, Vincent Bataille and Geneviève Mulak (French Society of Cardiology) for their assistance in designing the electronic case-record form and data management during the follow-up period.

AUTHOR CONTRIBUTIONS

Y.Z. and H.A-O. performed the experiments, acquired and interpreted the data. P.B. performed and interpreted the ultrasound studies. T.S. and N.D. were responsible for the FAST-MI cohort and interpreted the statistical data. A.P.S. contributed to the Baff/Baff-r studies. C.G. contributed to flow cytometry analysis and interpretation. J.V. and E.D. contributed to data acquisition and analysis. G.C. and L.L. performed the biomarkers measurements. D.T. and C.J.B. were involved in antibody measurements and anti-Baff experiments. S.K. performed the statistical analysis on the human data. P.B. analyzed and interpreted the disease pathology. I.F.C. provided the *Ccl7*$^{-/-}$ mice. A.T. contributed to study design and data interpretation. T.F.T. generated and provided the CD20 mAb. J-S.S. and Z.M. designed the experiments, analyzed and interpreted the data. Y.Z., J-S.S. and Z.M. wrote the manuscript.

COMPETING FINANCIAL INTERESTS

The authors have no conflicting financial interests to disclose.

FIGURE LEGENDS

Figure 1. The B cell depleting CD20 antibody reduces infarct size, improves heart function and limits myocardial inflammation. (a) Representative examples and quantitative analysis of $B220^{hi}$ IgM^{+} B cells staining in the blood of C57BL/6J mice treated with or without the CD20 antibody (anti-CD20) (*n* = 12 to 15 mice per group); *** $P < 0.001$. **(b)** Echocardiography analysis after anti-CD20 therapy. We measured LV shortening fraction (SF), LV internal diameter at end systole (LVIDs) and LV posterior wall thickness at end systole (LVPWs); * $P < 0.05$. **(c)** Representative photomicrographs and quantitative analysis of infarct size and myocardial fibrosis evaluation evaluated by Masson trichrome and Sirius Red stainings, respectively, in the 2 groups of mice. Data are representative of 10-14 mice per group in three independent experiments. Bars, upper panels, 1mm; lower panels,100 μm. **(d)** Representative histograms of mRNA levels of the pro-inflammatory cytokines IL-1β, TNF-α, IL-18 and the anti-inflammatory cytokines IL-10 and TGF-β, within the injured myocardium on day 14 after MI (*n* = 8-12 per group). Mean values ± SEM are represented. * $P < 0.05$; ** $P < 0.01$ vs PBS.

Figure 2. B lymphocyte depletion impairs monocyte mobilization, recruitment and macrophage accumulation in the injured myocardium. Representative examples of $7/4^{hi}$ and $7/4^{lo}$ monocyte stainings as well as quantification of their numbers in bone marrow **(a)** and blood **(b)** of B cell-depleted mice compared to controls on day 3 after MI (*n* = 8-15 per group). Mean values ± SEM are represented. * $P < 0.05$ vs PBS. **(c)** Quantitative analysis of $CD45.1^{+}$ $CD11b^{+}$ $Ly6G^{-}$ $Ly6C^{+}$ cells in the cardiac tissue of anti-CD20 treated animals compared to controls on day 3 after MI (*n* = 5 per group). **(d)**

Quantitative analysis of F4/80^{+} and CD68^{+} macrophages within the myocardium on day 5 post-MI (n = 5 per group). Mean values ± SEM are represented. * $P < 0.05$ vs PBS.

Figure 3. B lymphocyte depletion selectively reduces Ccl7 levels after acute MI and trigger Ccl7-dependent monocyte transmigration *in vitro and in vivo*. (a) Ccl2 and Ccl7 protein levels in blood after CD20 mAb treatment, 1 and 3 days after MI (n = 5-8 per group). **(b)** Bar graphs show Ccl7 release in the supernatant of non-stimulated or CpG-stimulated cultured B cells. Control ODN did not induce Ccl7 production (data not shown). **(c)** Representative photomicrographs and histograms of the transmigration of cultured monocytes in the presence of non-stimulated or activated (IgM and CD40) B cells with or without neutralizing anti-Ccl2 or anti-Ccl7 antibodies. Data are representative of four independent experiments, each condition was performed in triplicate. Bars, 300 μm. Mean values ± SEM are represented. * $P < 0.05$; *** $P < 0.001$ vs control. No cells could be counted when B cells were cultured in the absence of monocytes in the upper compartment, indicating no B cell contamination **(d)** Quantification of 7/4^{hi} monocytes in blood (left) and in the infarcted myocardium (right) of *Rag1*$^{-/-}$ mice injected with either wild-type splenocytes, B cell-depleted splenocytes, or B cell-depleted splenocytes re-supplemented with wild-type or *Ccl7*$^{-/-}$ B cells, 3 days after MI. Data are representative of 10 to 12 mice per group in two independent experiments. Mean values ± SEM are shown. * $P < 0.05$ vs WT splenocytes ; $^{\#\#}$ $P < 0.01$ vs anti-CD20 splenocytes; $^{\$}$ $P < 0.05$ vs anti-CD20 splenocytes with WT B cells.

Figure 4. B lymphocytes trigger adverse ventricular remodeling and alter heart function through the production of Ccl7. (a) Echocardiography analysis after 14 days of MI and assessment of LV shortening fraction (SF), LV internal diameter at end systole (LVIDs) and LV posterior wall thickness (LVPWs) of *Rag1*$^{-/-}$ mice injected with either wild-type splenocytes, B cell-depleted splenocytes, or B cell-depleted splenocytes re-supplemented with wild-type or *Ccl7*$^{-/-}$ B cells. **(b, c)** Representative photomicrographs and quantitative analysis of infarct size (**b**), fibrosis and collagen content (**c**) in the 4 groups of mice. Results are pooled from three independent experiments with 10 to 25 mice per group. Mean values ± SEM are shown. Bars, 1 mm in (**b**) and 100 µm in (**c**). * $P < 0.05$ and *** $P < 0.001$ vs WT splenocytes ; $^{\#}$ $P < 0.05$ and $^{\#\#\#}$ $P < 0.001$ vs α-CD20 splenocytes; $^{\$}$ $P < 0.05$ and $^{\$\$\$}$ $P < 0.001$ vs anti-CD20 splenocytes with WT B cells. **(d, e)** Restricted Ccl7 deficiency in B cells improved heart function after acute MI. **(d)** Quantitative analysis of circulating Ccl7 protein levels at day 14 post-MI in animals repopulated with a mixture of *µMT* and *Ccl7*$^{-/-}$ bone marrow compared to the control group receiving a mixture of *µMT* and *Ccl7*$^{+/+}$ bone marrow. **(e)** Quantitative analysis of the shortening fraction (%) at day 14 post-MI in the 2 groups of mice (n = 9 to 13 mice per group). Mean values ± SEM are shown. * $P < 0.05$.

Figure 5. Blockade of Baff signaling impairs monocyte mobilization and improves heart function after acute MI. (a) Quantification of the number of 7/4^{hi} monocytes in the bone marrow (left) and in the blood (right) of *Baff-r*$^{-/-}$ mice compared to controls on day 3 after MI. **(b)** Ccl7 protein levels in the plasma of *Baff-r*$^{-/-}$ mice compared to controls at day 3 post-MI. **(c)** Quantitative analysis of the shortening fraction (%) of *Baff-*

$r^{-/-}$ mice compared to *Baff*-$r^{+/+}$ and *Baff*-$r^{+/-}$ mice at day 14 post-MI. Data are representative of 8 to 11 mice per group. Mean values ± SEM are shown. * $P < 0.05$ and ** $P < 0.01$. **(d, e)** Quantification of the number of $B220^+$ IgM^+ B cells **(d)** and $7/4^{hi}$ monocytes **(e)** in blood of anti-Baff treated mice compared to PBS injected animals. **(f)** Quantitative analysis of the shortening fraction (%) of anti-Baff treated mice compared to PBS at day 14 post-MI (n = 12 to 15 mice per group). * $P < 0.05$, ** $P < 0.01$, *** $P < 0.001$.

Figure 6. Circulating levels of CCL7 and BAFF at the acute phase of MI are associated with cardiovascular outcomes. (a) The probability of outcome events (death or recurrent MI) as a function of baseline circulating CCL7 (**a**) or BAFF (**b**) level in patients with acute MI. Detectable CCL7 levels or high levels of BAFF at the admission for acute MI were independently predictive of death and recurrent MI after two years of follow-up after multiple adjustments (see Methods). HR= Hazard ratio.

REFERENCES

1. White, H.D. & Chew, D.P. Acute myocardial infarction. *Lancet* **372**, 570-584 (2008).
2. Jessup, M. & Brozena, S. Heart failure. *N Engl J Med* **348**, 2007-2018 (2003).
3. McMurray, J.J. & Pfeffer, M.A. Heart failure. *Lancet* **365**, 1877-1889 (2005).
4. Shah, A.M. & Mann, D.L. In search of new therapeutic targets and strategies for heart failure: recent advances in basic science. *Lancet* **378**, 704-712 (2011).
5. Nabel, E.G. & Braunwald, E. A tale of coronary artery disease and myocardial infarction. *N Engl J Med* **366**, 54-63 (2012).
6. Yellon, D.M. & Hausenloy, D.J. Myocardial reperfusion injury. *N Engl J Med* **357**, 1121-1135 (2007).
7. Taqueti, V.R., Mitchell, R.N. & Lichtman, A.H. Protecting the pump: controlling myocardial inflammatory responses. *Annu Rev Physiol* **68**, 67-95 (2006).
8. Zhang, M.*, et al.* Identification of a specific self-reactive IgM antibody that initiates intestinal ischemia/reperfusion injury. *Proc Natl Acad Sci U S A* **101**, 3886-3891 (2004).
9. Zhang, M.*, et al.* Identification of the target self-antigens in reperfusion injury. *J Exp Med* **203**, 141-152 (2006).
10. Zhang, M.*, et al.* Activation of the lectin pathway by natural IgM in a model of ischemia/reperfusion injury. *J Immunol* **177**, 4727-4734 (2006).
11. Haas, M.S.*, et al.* Blockade of self-reactive IgM significantly reduces injury in a murine model of acute myocardial infarction. *Cardiovasc Res* **87**, 618-627 (2010).

12. Renner, B.*, et al.* B cell subsets contribute to renal injury and renal protection after ischemia/reperfusion. *J Immunol* **185**, 4393-4400 (2010).

13. Pepys, M.B.*, et al.* Targeting C-reactive protein for the treatment of cardiovascular disease. *Nature* **440**, 1217-1221 (2006).

14. Salio, M.*, et al.* Cardioprotective function of the long pentraxin PTX3 in acute myocardial infarction. *Circulation* **117**, 1055-1064 (2008).

15. Granger, D.N. & Korthuis, R.J. Physiologic mechanisms of postischemic tissue injury. *Annu Rev Physiol* **57**, 311-332 (1995).

16. Vinten-Johansen, J. Involvement of neutrophils in the pathogenesis of lethal myocardial reperfusion injury. *Cardiovasc Res* **61**, 481-497 (2004).

17. Nahrendorf, M.*, et al.* The healing myocardium sequentially mobilizes two monocyte subsets with divergent and complementary functions. *J Exp Med* **204**, 3037-3047 (2007).

18. Leuschner, F.*, et al.* Rapid monocyte kinetics in acute myocardial infarction are sustained by extramedullary monocytopoiesis. *J Exp Med* **209**, 123-137 (2012).

19. Mahaffey, K.W.*, et al.* Effect of pexelizumab, an anti-C5 complement antibody, as adjunctive therapy to fibrinolysis in acute myocardial infarction: the COMPlement inhibition in myocardial infarction treated with thromboLYtics (COMPLY) trial. *Circulation* **108**, 1176-1183 (2003).

20. Granger, C.B.*, et al.* Pexelizumab, an anti-C5 complement antibody, as adjunctive therapy to primary percutaneous coronary intervention in acute myocardial infarction: the COMplement inhibition in Myocardial infarction treated with Angioplasty (COMMA) trial. *Circulation* **108**, 1184-1190 (2003).

21. Armstrong, P.W.*, et al.* Pexelizumab for acute ST-elevation myocardial infarction in patients undergoing primary percutaneous coronary intervention: a randomized controlled trial. *JAMA* **297**, 43-51 (2007).

22. Eikelboom, J.W. & O'Donnell, M. Pexelizumab does not "complement" percutaneous coronary intervention in patients with ST-elevation myocardial infarction. *JAMA* **297**, 91-92 (2007).

23. Martin, F. & Chan, A.C. B cell immunobiology in disease: evolving concepts from the clinic. *Annu Rev Immunol* **24**, 467-496 (2006).

24. Uchida, J.*, et al.* Mouse CD20 expression and function. *Int Immunol* **16**, 119-129 (2004).

25. Ait-Oufella, H.*, et al.* B cell depletion reduces the development of atherosclerosis in mice. *J Exp Med* **207**, 1579-1587 (2010).

26. Hamaguchi, Y.*, et al.* The peritoneal cavity provides a protective niche for B1 and conventional B lymphocytes during anti-CD20 immunotherapy in mice. *J Immunol* **174**, 4389-4399 (2005).

27. Busche, M.N., Pavlov, V., Takahashi, K. & Stahl, G.L. Myocardial ischemia and reperfusion injury is dependent on both IgM and mannose-binding lectin. *Am J Physiol Heart Circ Physiol* **297**, H1853-1859 (2009).

28. Tsou, C.L.*, et al.* Critical roles for CCR2 and MCP-3 in monocyte mobilization from bone marrow and recruitment to inflammatory sites. *J Clin Invest* (2007).

29. Mackay, F. & Schneider, P. Cracking the BAFF code. *Nat Rev Immunol* **9**, 491-502 (2009).

30. Kelly-Scumpia, K.M.*, et al.* B cells enhance early innate immune responses during bacterial sepsis. *J Exp Med* **208**, 1673-1682 (2011).

31. Rauch, P.J.*, et al.* Innate response activator B cells protect against microbial sepsis. *Science* **335**, 597-601 (2012).

32. Yilmaz, G., Arumugam, T.V., Stokes, K.Y. & Granger, D.N. Role of T lymphocytes and interferon-gamma in ischemic stroke. *Circulation* **113**, 2105-2112 (2006).

33. Burne-Taney, M.J.*, et al.* B cell deficiency confers protection from renal ischemia reperfusion injury. *J Immunol* **171**, 3210-3215 (2003).

34. Jang, H.R.*, et al.* B cells limit repair after ischemic acute kidney injury. *J Am Soc Nephrol* **21**, 654-665 (2010).

35. Goodchild, T.T.*, et al.* Bone marrow-derived B cells preserve ventricular function after acute myocardial infarction. *JACC Cardiovasc Interv* **2**, 1005-1016 (2009).

36. Kyaw, T.*, et al.* Conventional B2 B cell depletion ameliorates whereas its adoptive transfer aggravates atherosclerosis. *J Immunol* **185**, 4410-4419 (2010).

37. Sage, A.P.*, et al.* BAFF receptor deficiency reduces the development of atherosclerosis in mice--brief report. *Arterioscler Thromb Vasc Biol* **32**, 1573-1576 (2012).

38. Kyaw, T.*, et al.* Depletion of B2 but not B1a B cells in BAFF receptor-deficient ApoE mice attenuates atherosclerosis by potently ameliorating arterial inflammation. *PLoS One* **7**, e29371 (2012).

39. Yanaba, K.*, et al.* B-lymphocyte contributions to human autoimmune disease. *Immunol Rev* **223**, 284-299 (2008).

ONLINE METHODS

Myocardial infarction. All mice were on full C57Bl/6J background. C57BL/6 (Janvier, France), *Ccl7*$^{-/-}$ [28], *Baff-r*$^{-/-}$, *Rag1*$^{-/-}$, CD45.1 mice (The Jackson Laboratory) and *Myd88*$^{-/-}$ *Trif*$^{-/-}$ mice (provided by Ryffel B [40]) were 8 weeks old. Myocardial infarction was induced by left coronary ligation [41]. Mice were anesthetized using ketamine (870 mg kg^{-1}) and xylazine (140 mg kg^{-1}) via intraperitoneal injection (i.p.), then intubated and ventilated with air using a small animal respirator. The chest wall was shaved and a thoracotomy was performed in the fourth left intercostal space. The left ventricle was visualized, the pericardial sac was then removed and the left anterior descending artery was permanently ligated using a 7/0 monofilament suture (Péters surgical, France) at the site of its emergence from under the left atrium. Significant color changes at the ischemic area were considered indicative of successful coronary occlusion. The thoracotomy was closed with 6/0 monofilament sutures. The same procedure was performed for sham-operated control animals except that the ligature was left untied. The endotracheal tube was removed once spontaneous respiration resumed, and animals were placed on a warm pad maintained at 37 °C until the mice were completely awake. One hour after myocardial infarction induction, mice were treated i.p. with a mouse monoclonal CD20 antibody (200 µg/mouse) [24,25], with an anti-Baff antibody (clone 10F4, 100 µg/mouse, repeated at day1 after MI) [42] or with PBS. In leukocytes recruitment experiments, CD20 mAb-treated mice or untreated group received both 15 x 10^6 CD45.1$^+$ bone marrow mononuclear-derived cells 4 hours after MI. In other sets of experiments, 7 days before myocardial infarction induction, *Rag1*$^{-/-}$ mice received either 2 x 10^7 wild-

type splenocytes, 1.2 x 10^7 B cell-depleted splenocytes recovered from CD20 mAb-treated mice, B cell-depleted splenocytes re-supplemented with 8 x 10^6 wild-type B lymphocytes or with 8 x 10^6 *Ccl7*$^{-/-}$ B lymphocytes. In additional experiments, we generated a B cell-restricted *Ccl7*-deficient mouse model by reconstituting lethally-irradiated wild-type animals with a mixture of *μMT* and *Ccl7*$^{-/-}$ bone marrow as previously described [31,37]. In this case, all reconstituted B cells originate from *Ccl7*$^{-/-}$ bone marrow and are therefore completely deficient in *Ccl7*. The control group received a mixture of *μMT* and *Ccl7*$^{+/+}$ bone marrow. Mice were allowed to recover for 5 weeks. Experiments were conducted according to the French veterinary guidelines and those formulated by the European Community for experimental animal use, and were approved by the Institut National de la Santé et de la Recherche Médicale.

Echocardiographic measurements. Transthoracic echocardiography was performed 14 days after surgery using an echocardiograph (ACUSON S3000™ ultrasound, Siemens AG, Erlangen Germany) equipped with a 14-MHz linear transducer (1415SP). The investigator was blinded to group assignment. Animals were anesthetized by isoflurane inhalation. Two-dimensional parasternal long-axis views of the left ventricle were obtained for guided M-mode measurements of the LV internal diameter at end diastole (LVDD) and end systole (LVDS), as well as the interventricular septal wall thickness, and posterior wall thickness at the same points. Percent fractional shortening (%FS) were calculated by the following formulas: %FS = [(LVDD - LVDS)/LVDD] X 100.

Histopathological analysis. Cardiac healing following myocardial infarction was

assessed at day 14. Hearts were excised, rinsed in PBS and frozen in liquid nitrogen. Hearts were cut by a cryostat (CM 3050S, Leica) into 7-μm-thick sections. Masson's trichrome and Sirius Red stainings were performed for infarct size and myocardial fibrosis evaluation. Infarct size (in percent) was calculated as total infarct circumference divided by total LV circumference. The collagen volume fraction was calculated as the ratio of the total area of interstitial fibrosis to the myocyte area in the entire visual field of the section. B lymphocyte immunostaining was performed according to an indirect immunoperoxidase method using an anti-CD45R/B220 antibody (RA3-6B2, Southern Biotechnology) and AEC substrate kit (Dako). Endothelial cells forming capillaries were visualized after BS-1 lectin staining (FITC conjugated Griffonia simplicifolia, Sigma-Aldrich) and arterioles using an anti-α-actin smooth muscle antibody (Abcam).

Cells. Mice were killed at 12 h and on days 1, 3, 5, 7 and 14 after myocardial infarction (n = 5-10 mice per time point). Peripheral blood was drawn via inferior vena cava puncture with heparin solution. Whole blood was lysed after immunofluoresence staining using the BD FACS lysing solution and total blood leukocyte numbers were determined using Trypan Blue. Spleens were removed and bone marrow cells were drawn from femur and tibia and filtered through 40 μm nylon mesh (BD Biosciences). The cell suspension was centrifuged at 400 g for 10 min at 4 °C. Red blood cells were lysed (Sigma-Aldrich) and splenocytes and bone marrow cells were washed with PBS supplemented with 3% FBS. Infarct tissue and healthy hearts were harvested, minced with fine scissors, and placed into a cocktail of Collagenase I (450 U ml^{-1}), Collagenase XI (125 U ml^{-1}), DNase I (60 U ml^{-1}), and Hyaluronidase (60 U ml^{-1}) (sigma-Aldrich)

and shaken at 37 °C for 1 h. Cells were then triturated through nylon mesh (40 μm) and centrifuged (10 min, 400 g, 4 °C). Mononuclear cells were purified by density centrifugation (25 min, 400 g, room temperature). The resulting cell suspensions were washed and total leukocyte numbers were determined.

Cell purification, culture and transmigration assay. B cells were isolated from C57BL/6J spleens using a B cell isolation kit (Miltenyi Biotec) according to the manufacturer's protocol. B cells were stimulated during 48 h with 10 μg ml^{-1} of anti–mouse IgM (Jackson ImmunoResearch Laboratories, Inc.) and 2.5 μg ml^{-1} of anti–mouse CD40 (clone HM40-3, BioLegend). Monocytes were isolated from bone marrow. Bone marrow fraction was enriched by neutrophils depletion using autoMACS columns (Miltenyi) and anti-Ly6G magnetic beads. $7/4^{hi}$ monocytes (7/4 staining is equivalent to Ly6C staining [43]) were then sorted on a FACSAria (BD Biosciences). *In vitro* monocytes transmigration was performed over cell culture inserts (Millicell-PCF, Millipore) with porous polycarbonate filters (8 μm pore size) in 24-well plates. Inserts were coated with rat-tail type I collagen (60 μg ml^{-1}) for 30min at 37°C, then blocked with 3% BSA in PBS for 1 h at 37 °C. We used 300 μL of RPMI-FBS 10% containing 2 x 10^6 of B lymphocytes in the lower compartment and 200 μL containing 9 x 10^4 of $7/4^{hi}$ monocytes were added to the upper compartment. Two μg ml^{-1} of Ccl7-specific neutralizing antibody or 1 μg ml^{-1} of Ccl2 neutralizing antibody (R&D systems) were added in the lower compartment before migration. Monocytes were allowed to migrate for 4 h at 37 °C. The filters were then washed with PBS, and fixed in 1% paraformaldehyde. The upper surfaces of the filters were scraped with cotton swabs to remove the non-migrating

cells. The filters were then stained with DAPI (Sigma-Aldrich). Migrating cells attached to the lower surfaces of the filters were visualized under an Axioimager Z1 microscope (Zeiss). Each experiment was performed in triplicate.

Flow Cytometry. The following antibodies were used: FITC-conjugated anti-CD11b (M1/70, BD Pharmingen), PE-conjugated anti-Ly6G (1A8, BD Pharmingen), PE-conjugated anti-NK-1.1 (PK 136, BD Pharmingen), APC-conjugated anti-Ly-6B.2 (7/4, AbD Serotec), APC-conjugated anti-CD3e (17A2, eBioscience), FITC-conjugated anti-CD4 (RM 4-5, eBioscience), PercP-conjugated anti-CD8a (53-6.7, BD Pharmingen), PE-conjugated anti-CD45R/B220 (RA3-6B2, eBioscience), APC-conjugated anti-IgM (II/41, eBioscience), PE-Cy7-conjugated anti-CD11c (N418, eBioscience), APC-conjugated anti-CD19 (BD Pharmingen), V450-conjugated anti-IgD (BD Horizon), APC-conjugated anti-CD21 (BD Pharmingen), PE-conjugated anti-CD23 (BD Pharmingen), biotinylated anti-Ccl7 (PeproTech), and APC-conjugated anti-CD45.1 (A20, BD Pharmingen). Monocytes were identified as $CD11b^{hi}$ $Ly6G^{-}$ $7/4^{hi/lo}$. Neutrophils were identified as $CD11b^{+}$ $Ly6G^{hi}$ $7/4^{hi}$. Macrophages/dendritic cells were identified as $CD11c^{hi}$. NK cells were identified as $CD11b^{+}$ $Ly6G^{-}$ $7/4^{-}$ $NK1.1^{+}$. Mature B lymphocytes were identified as $B220^{hi}$ IgM^{hi}. Normalization to weight of infarct was performed for total cell numbers determination in the heart. Cells were analyzed using a flow cytometer (LSR II, BD).

Antibody measurements. Circulating IgM, IgG1, and IgG2c levels were measured in plasma of treated mice at indicated time points using a chemiluminescent-based sandwich ELISA.

Quantitative real-time PCR. Quantitative real-time PCR was performed on a Step-one Plus (Applied Biosystems). GAPDH was used to normalize gene expression. The following primer sequence were used: forward 5'-CGT-CCCGTAGACAAAATGGTGAA-3', reverse 5'-GCCGTGAGTGGAGTCATACTGGAA-CA-3' ; IL1β : forward 5'-GAAGAGCCCATCCTCTGTGA-3', reverse 5'-GGGTGTGCCGTCTTTCATTA-3'; TNF-α : forward 5'-GATGGGGGGCTTCCAGAACT-3', reverse 5'-GATGGGGGGCTTCCAGAACT-3' ; IL-18 : forward 5'-AGTGAACCCCAGACCAGACTGA-3', reverse 5'-CCCTCCCCACCTAACTTTGATGTA-3' ; TGF-β : forward 5'-CGGAGAGCCCTGGATACCAACTA-3', reverse 5'-GCCGCACACAGCAGTTCTTCTCT-3'.

Chemokines levels. Plasma and/or heart levels of Ccl2, Ccl12, Cxcl13 and Ccl7 were measured using Quantikine Elisa Kits (R&D Systems and PeproThec, respectively) according to the manufacturer's instructions.

Population of patients with acute MI. The population and methods of the French registry of Acute ST-elevation and non–ST-elevation Myocardial Infarction (FAST-MI) have been described in detail in previous publications [44]. Briefly, all patients ≥ 18 years of age were included in the registry if they had elevated serum markers of myocardial necrosis higher than twice the upper limit of normal for creatine kinase, creatine kinase-

MB or elevated troponins, and either symptoms compatible with acute MI and/or electrocardiographic changes on at least two contiguous leads with pathologic Q waves (≥ 0·04 sec) and/or persisting ST elevation or depression > 0·1 mV. The time from symptom onset to intensive care unit admission had to be < 48 h. Patients were managed according to usual practice; treatment was not affected by participation in the registry. Of the 374 centers in France that treated patients with acute MI at that time, 223 (60%) participated in the registry. Among these, 100 centers recruited 1,029 patients who contributed to a serum bank. For the present study, 1,000 samples were available for CCL7 measurement and 959 samples were available for BAFF measurement. Written informed consent was provided by each patient. Their baseline characteristics were comparable to the overall population of the registry. More than 99% of patients were Caucasians. Follow-up was collected through contacts with the patients' physicians, the patients themselves or their family, and registry offices of their birthplace. One-year follow-up was > 99% complete. The study was reviewed by the Committee for the Protection of Human Subjects in Biomedical Research of Saint Antoine University Hospital and the data file was declared to the Commission Nationale Informatique et Liberté. Human CCL7 analysis was carried out using the Bioplex Pro magnetic technology (Bio-Plex Pro™ Human Cytokine CCL7 Set #171-B6012M, Bio-Rad), following the manufacturer's instructions. Frozen (−80 °C) EDTA plasma samples from each patient were all analyzed on the same day. Samples were thawed and spun at 2,500 g for 15 min at room temperature prior to use and particle clear plasma was used at 1:4 dilution. Data were acquired on 50 beads/patient and analyzed following a 1:4 serial dilution standard curve (concentration in range = 0.33-3472 pg ml^{-1}) using the Bio-Plex

Manager 6.1 Software and 5PL logistic regression (FitProb. = 0.0000, ResVar. = 7.7585). Baff was measured using Quantikine Human Baff Immunoassay (ref SBLYS0, R&D Systems) following manufacturer's instructions. The limit of detection was 3.38 pg ml^{-1}.

Statistical analysis. Results were expressed as mean ± SEM. Kruskal-Wallis was used to compare each parameter. Post hoc Mann–Whitney *U* tests with Bonferroni correction were then performed to identify which group differences accounted for the significant overall Kruskal-Wallis result. Statistical analysis in FAST-MI was conducted as follows. An outcome event was defined as all-cause death or non-fatal MI during the one-year follow-up period. The primary endpoint was defined as a composite of all-cause death and non-fatal MI, and was adjudicated by a committee whose members were unaware of patients' medications, and blood measurements. Continuous variables are described as mean ± SD and categorical variables as frequencies and percentages. Baseline demographic and clinical characteristics, treatment factors, and therapeutic management during hospitalisation were compared among patients with or without detectable circulating CCL7 levels using chi-square or Fisher' s exact tests for discrete variables, and by unpaired T tests, Wilcoxon sign-rank tests for continuous variables. Survival curves according to detectable or undetectable CCL7 levels are estimated using the Kaplan Meier estimator. We used a multivariable Cox proportional-hazards model to assess the independent prognostic value of variables with the primary endpoint during the 1-year follow-up period. The multivariable model comprised sex, age, previous or current smoking, family history of coronary disease, history of hypertension, previous MI, heart failure, renal failure, diabetes, heart rate at admission, Killip class, left ventricular

ejection fraction, hospital management (including reperfusion therapy, statins, beta-blockers, clopidogrel, diuretics, digitalis, heparin), troponin I and log CRP levels. Results are expressed as hazard ratios for Cox models with 95% confidence intervals (CIs). All statistical tests were two-sided and performed using SAS software version 9.1.

40. Togbe, D.*, et al.* Nonredundant roles of TIRAP and MyD88 in airway response to endotoxin, independent of TRIF, IL-1 and IL-18 pathways. *Lab Invest* **86**, 1126-1135 (2006).

41. Kumar, D.*, et al.* Distinct mouse coronary anatomy and myocardial infarction consequent to ligation. *Coron Artery Dis* **16**, 41-44 (2005).

42. Scholz, J.L.*, et al.* BLyS inhibition eliminates primary B cells but leaves natural and acquired humoral immunity intact. *Proc Natl Acad Sci U S A* **105**, 15517-15522 (2008).

43. Cochain, C.*, et al.* Regulation of monocyte subset systemic levels by distinct chemokine receptors controls post-ischaemic neovascularization. *Cardiovasc Res* **88**, 186-195 (2010).

44. Simon, T.*, et al.* Genetic determinants of response to clopidogrel and cardiovascular events. *N Engl J Med* **360**, 363-375 (2009).

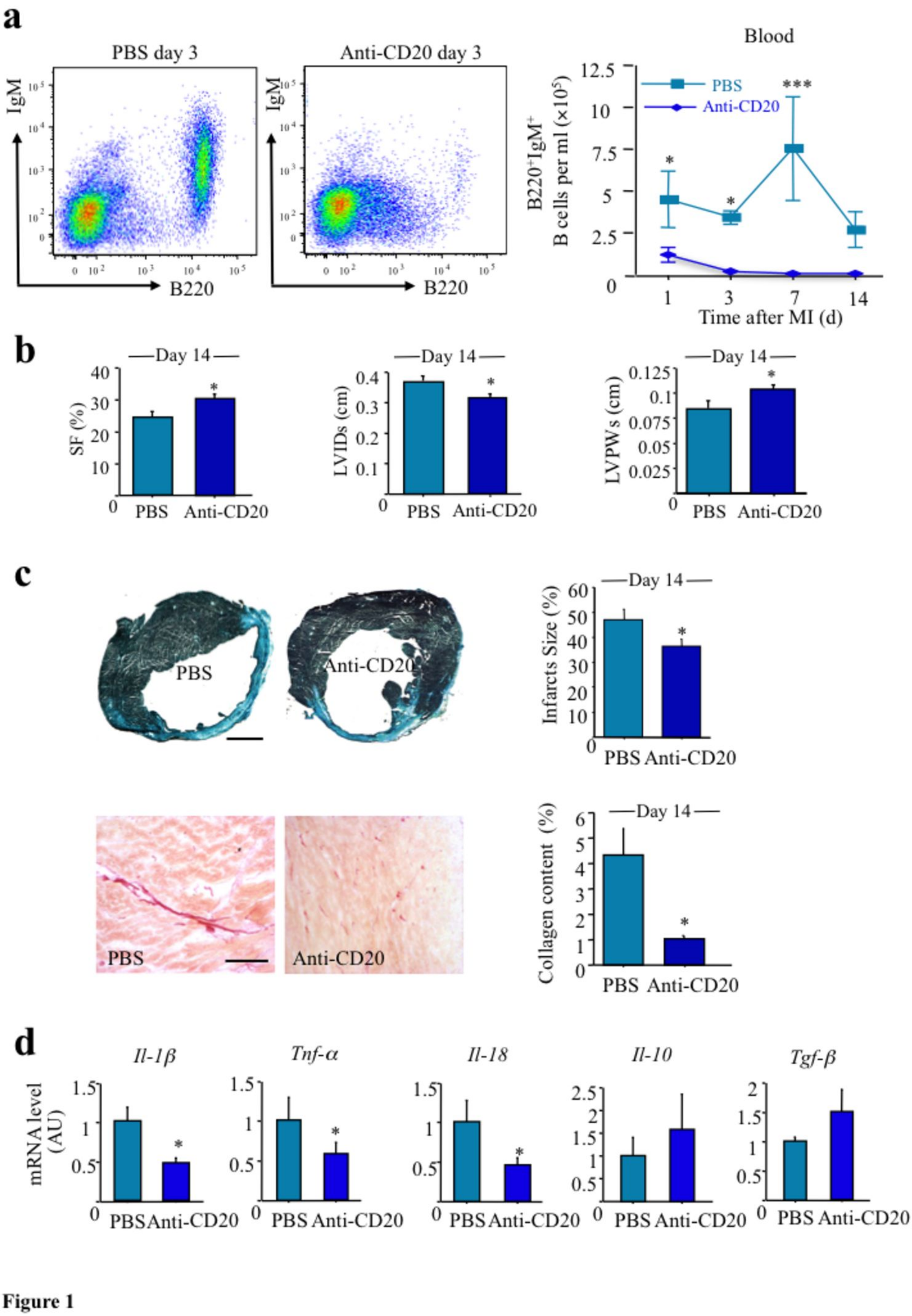
a
PBS day 3
Anti-CD20 day 3
IgM
B220
Blood
B220+IgM+ B cells per ml (×10^5)
PBS
Anti-CD20
Time after MI (d)
b
Day 14
SF (%)
LVIDs (cm)
LVPWs (cm)
PBS
Anti-CD20
c
Infarcts Size (%)
Collagen content (%)
d
Il-1β
Tnf-α
Il-18
Il-10
Tgf-β
mRNA level (AU)

Figure 1

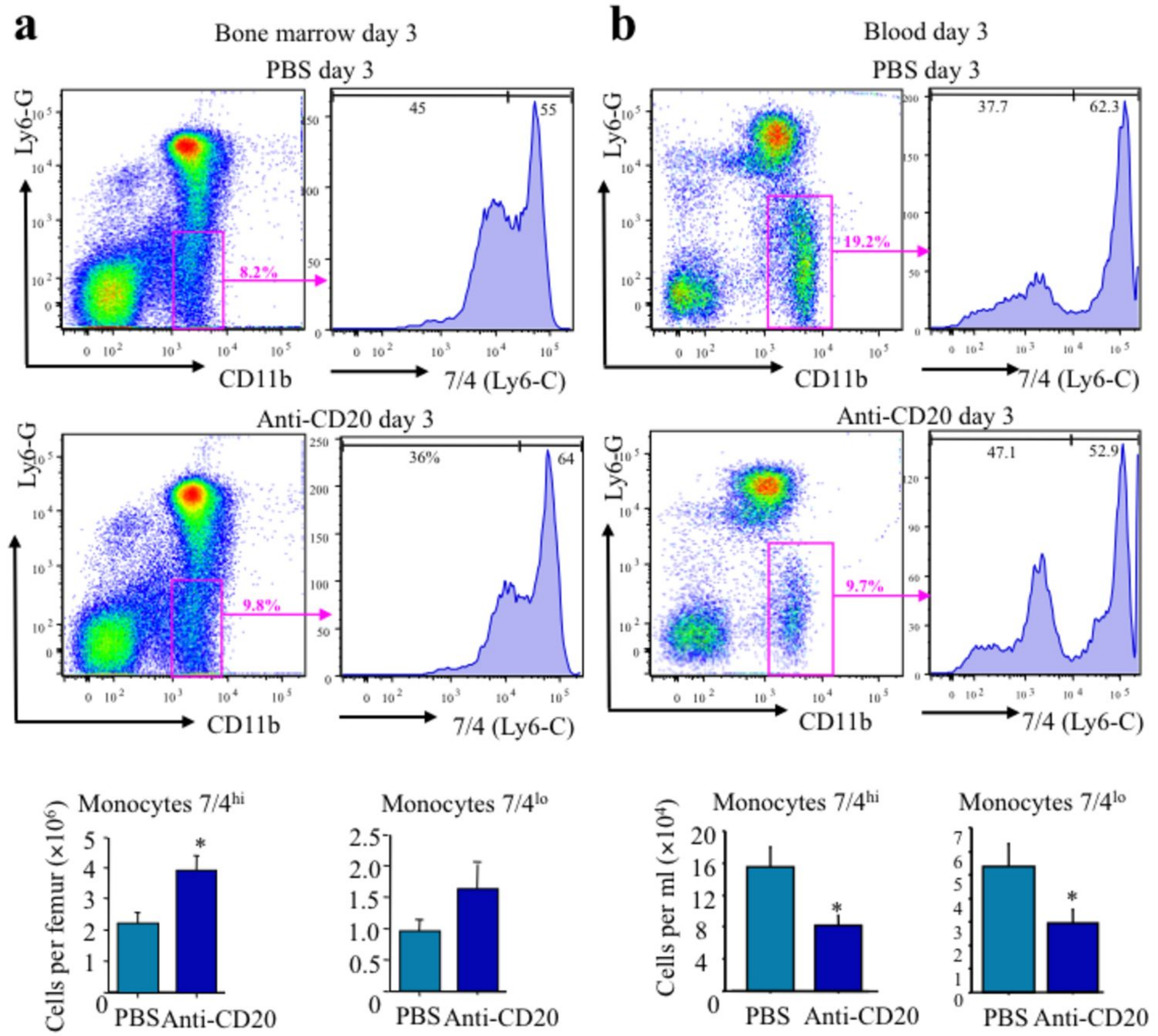
a
Bone marrow day 3
PBS day 3
Ly6-G
CD11b
8.2%
45
55
7/4 (Ly6-C)
Anti-CD20 day 3
9.8%
36%
64
b
Blood day 3
PBS day 3
19.2%
37.7
62.3
Anti-CD20 day 3
9.7%
47.1
52.9
Monocytes 7/4hi
Cells per femur (×10⁶)
PBS Anti-CD20
Monocytes 7/4lo
Cells per ml (×10⁴)

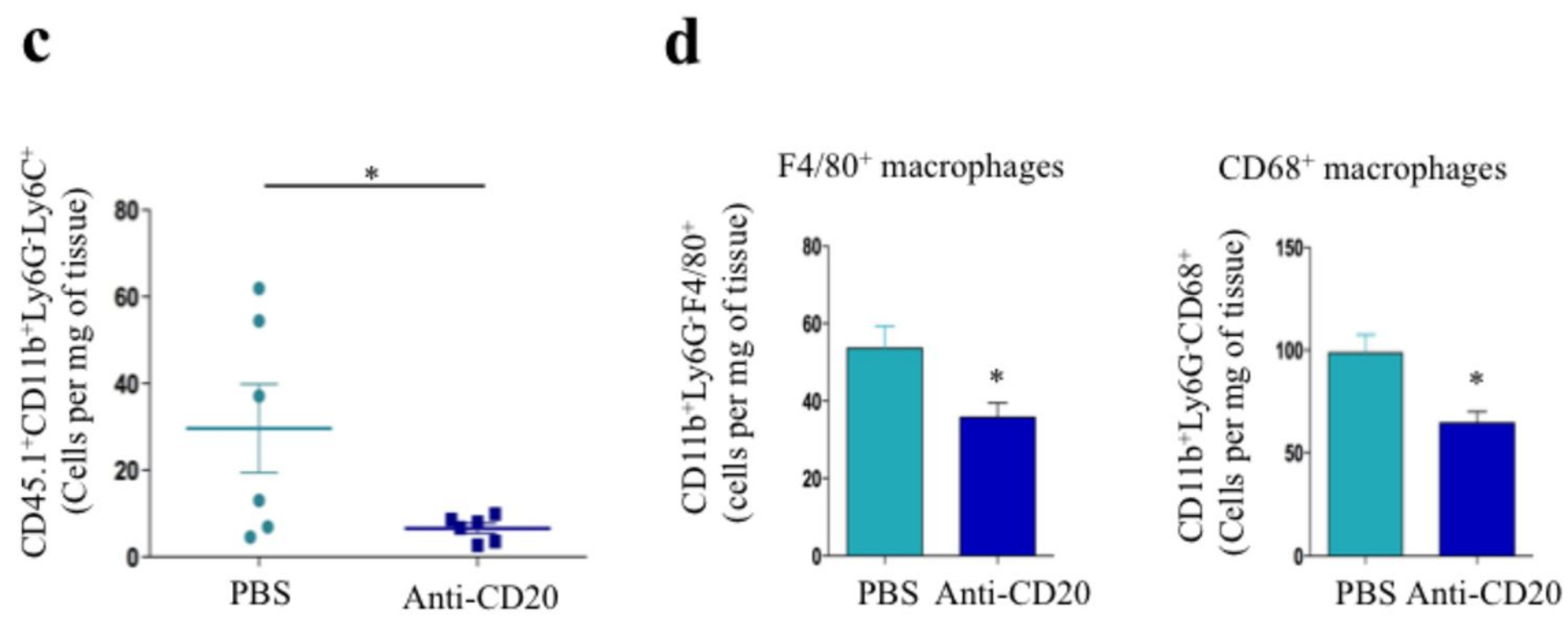
c
CD45.1+CD11b+Ly6G-Ly6C+
(Cells per mg of tissue)
PBS
Anti-CD20
d
F4/80+ macrophages
CD11b+Ly6G-F4/80+
(cells per mg of tissue)
CD68+ macrophages
CD11b+Ly6G-CD68+
(Cells per mg of tissue)

Figure 2

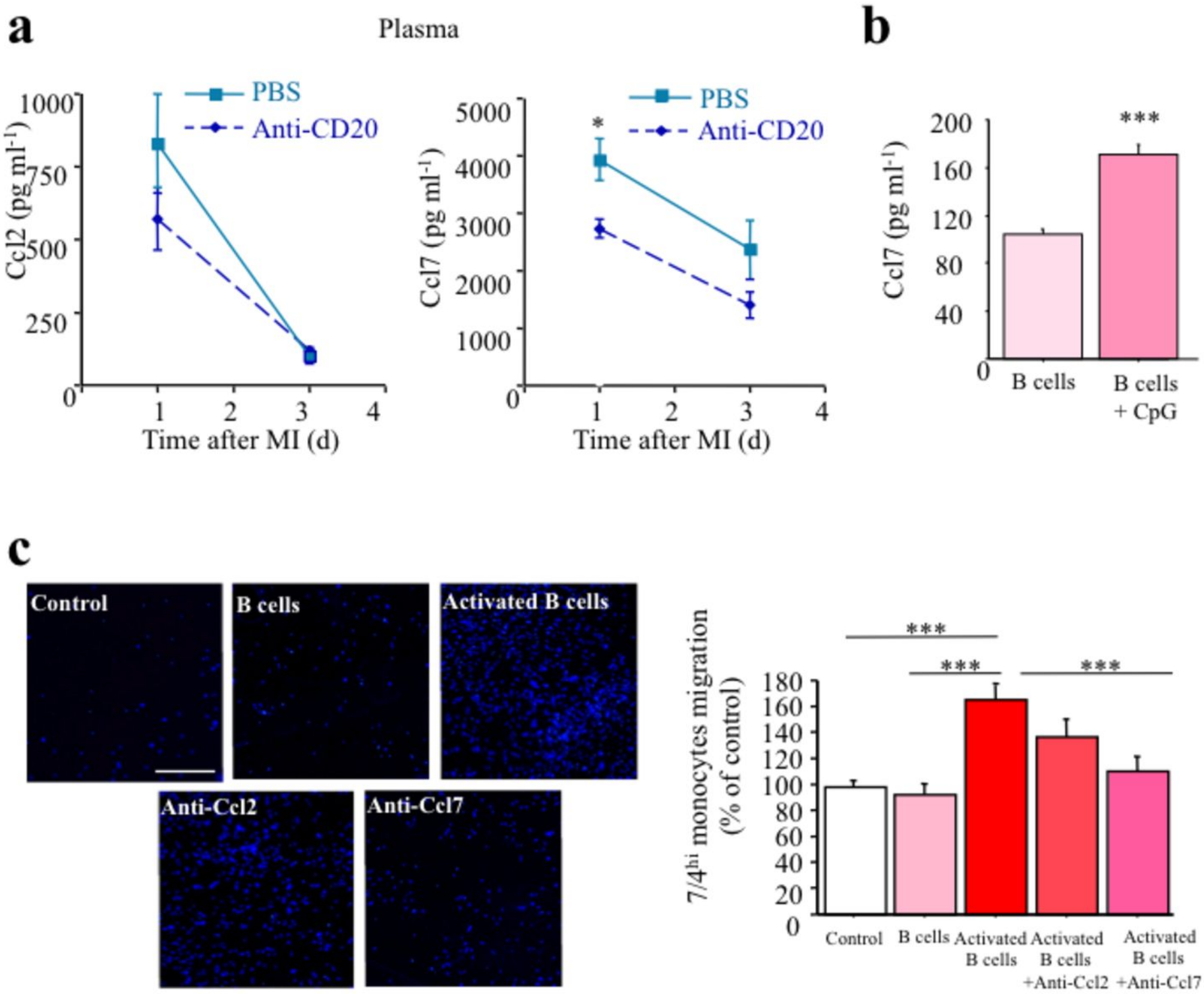
a
Plasma
PBS
Anti-CD20
Ccl2 (pg ml-1)
1000
750
500
250
0
1
2
3
4
Time after MI (d)
PBS
Anti-CD20
Ccl7 (pg ml-1)
5000
4000
3000
2000
1000
0
*
1
2
3
4
Time after MI (d)
b
Ccl7 (pg ml-1)
200
160
120
80
40
0
***
B cells
B cells
+ CpG
c
Control
B cells
Activated B cells
Anti-Ccl2
Anti-Ccl7
7/4hi monocytes migration
(% of control)
180
160
140
120
100
80
60
40
20
0
***
***
***
Control
B cells
Activated B cells
Activated B cells +Anti-Ccl2
Activated B cells +Anti-Ccl7
d
Spleno WT
Spleno Anti-CD20
Spleno Anti-CD20 +WT B cells
Spleno Anti-CD20 +Ccl7-/- B cells
Blood day 3
Cells per ml (×10⁴)
40
35
30
25
20
15
10
5
0
*
Heart day 3
Percentage of CD11b+ 7/4hi monocytes
80
70
60
50
40
30
20
10
0
*
##
$

Figure 3

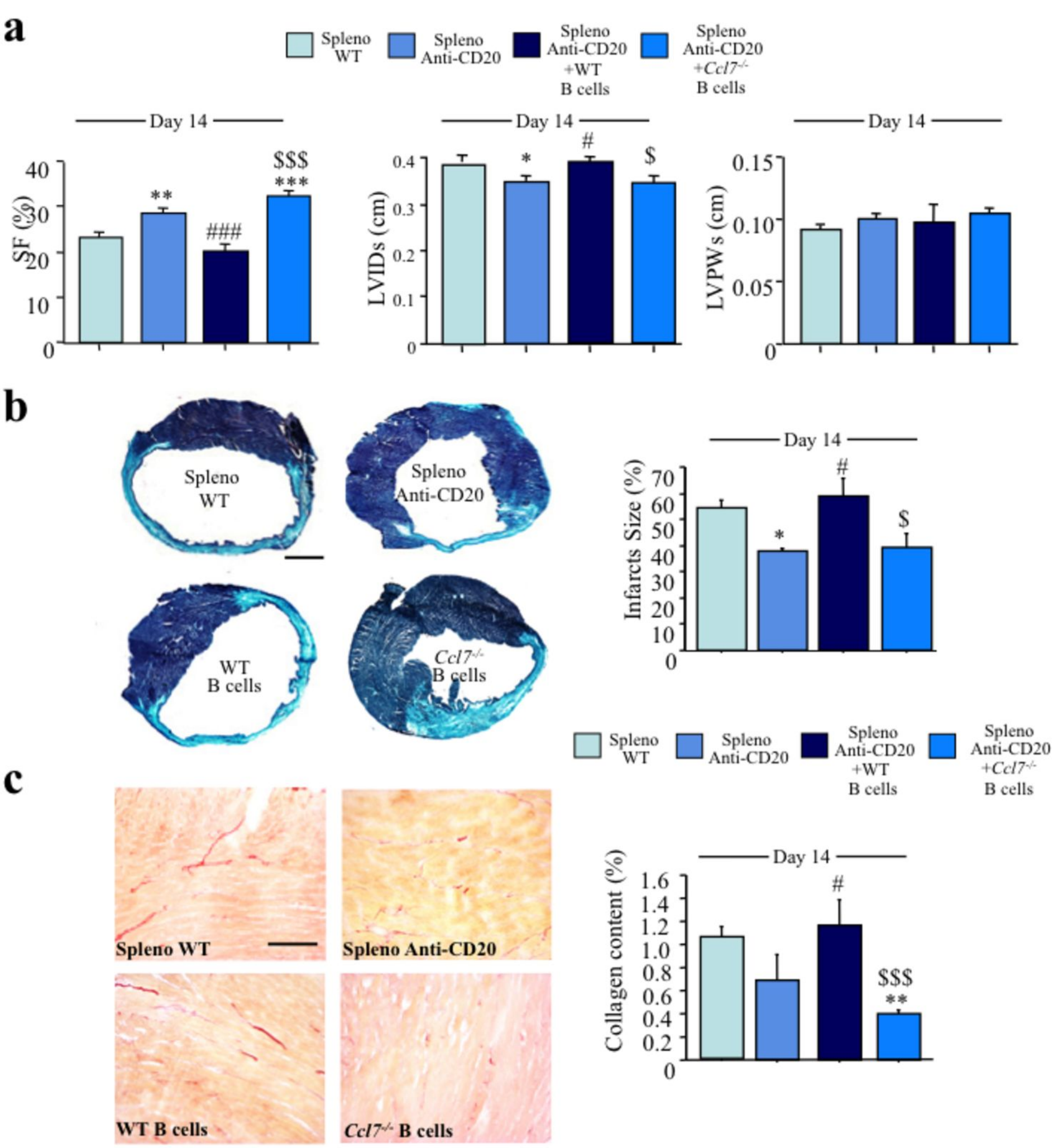
a
Spleno WT
Spleno Anti-CD20
Spleno Anti-CD20 +WT B cells
Spleno Anti-CD20 +Ccl7-/- B cells
Day 14
SF (%)
LVIDs (cm)
LVPWs (cm)
b
Spleno WT
Spleno Anti-CD20
WT B cells
Ccl7-/- B cells
Infarcts Size (%)
c
Spleno WT
Spleno Anti-CD20
WT B cells
Ccl7-/- B cells
Collagen content (%)
d
Day14
Ccl7 (pg ml-1)
µMT +Ccl7+/+
µMT +Ccl7-/-
e
SF (%)

Figure 4

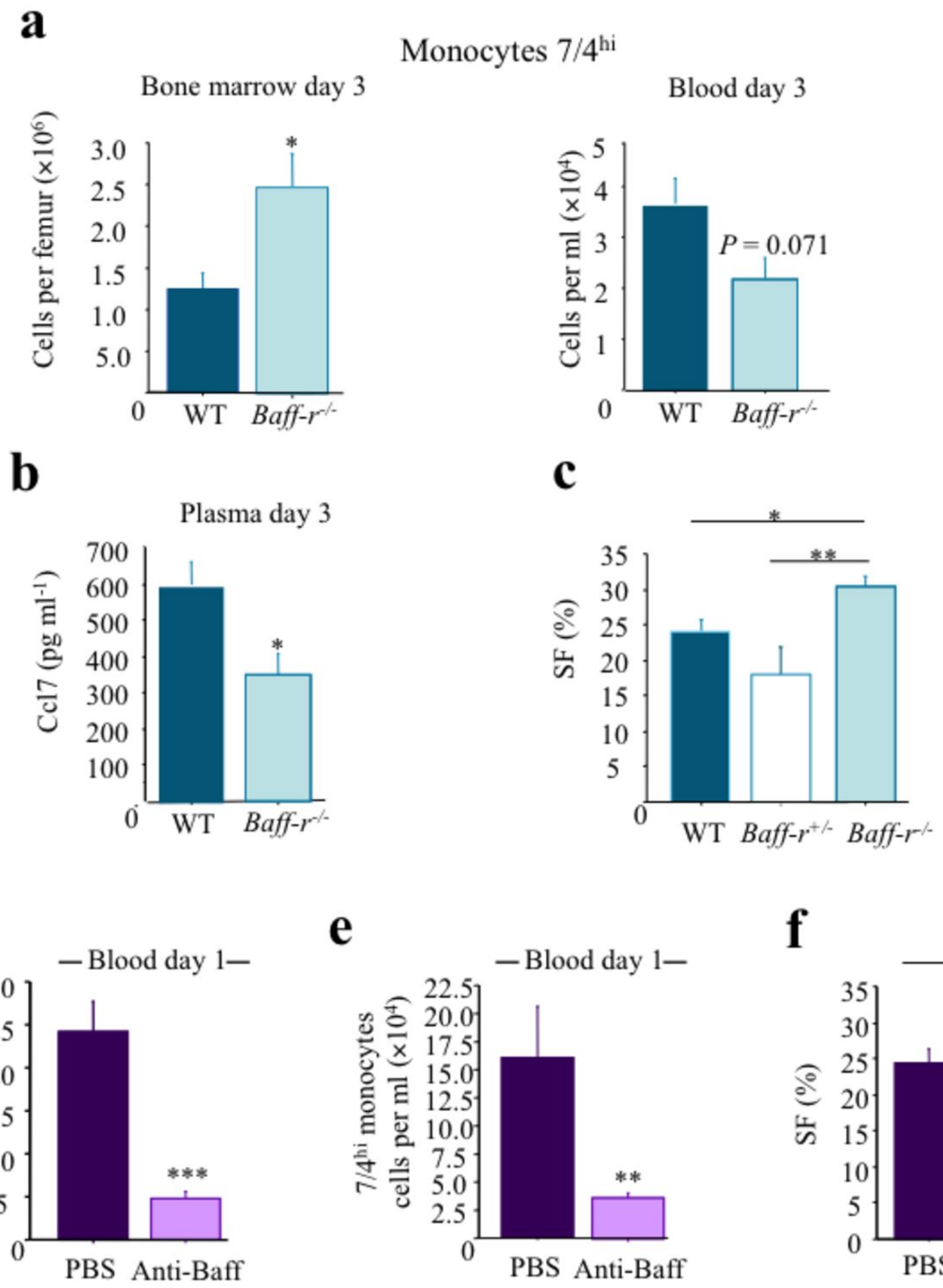
a
Monocytes 7/4hi
Bone marrow day 3
Cells per femur (×10⁶)
3.0
2.5
2.0
1.5
1.0
5.0
0
WT
Baff-r-/-
Blood day 3
Cells per ml (×10⁴)
5
4
3
2
1
0
P = 0.071
WT
Baff-r-/-
b
Plasma day 3
Ccl7 (pg ml-1)
700
600
500
400
300
200
100
0
WT
Baff-r-/-
c
SF (%)
35
30
25
20
15
10
5
0
WT
Baff-r+/-
Baff-r-/-
d
— Blood day 1 —
B cells per ml (×10⁴)
30
25
20
15
10
5
0
PBS
Anti-Baff
e
— Blood day 1 —
7/4hi monocytes cells per ml (×10⁴)
22.5
20.0
17.5
15.0
12.5
10.0
7.5
5.0
2.5
0
PBS
Anti-Baff
f
— Day 14 —
SF (%)
35
30
25
20
15
10
5
0
PBS
Anti-Baff

Figure 5

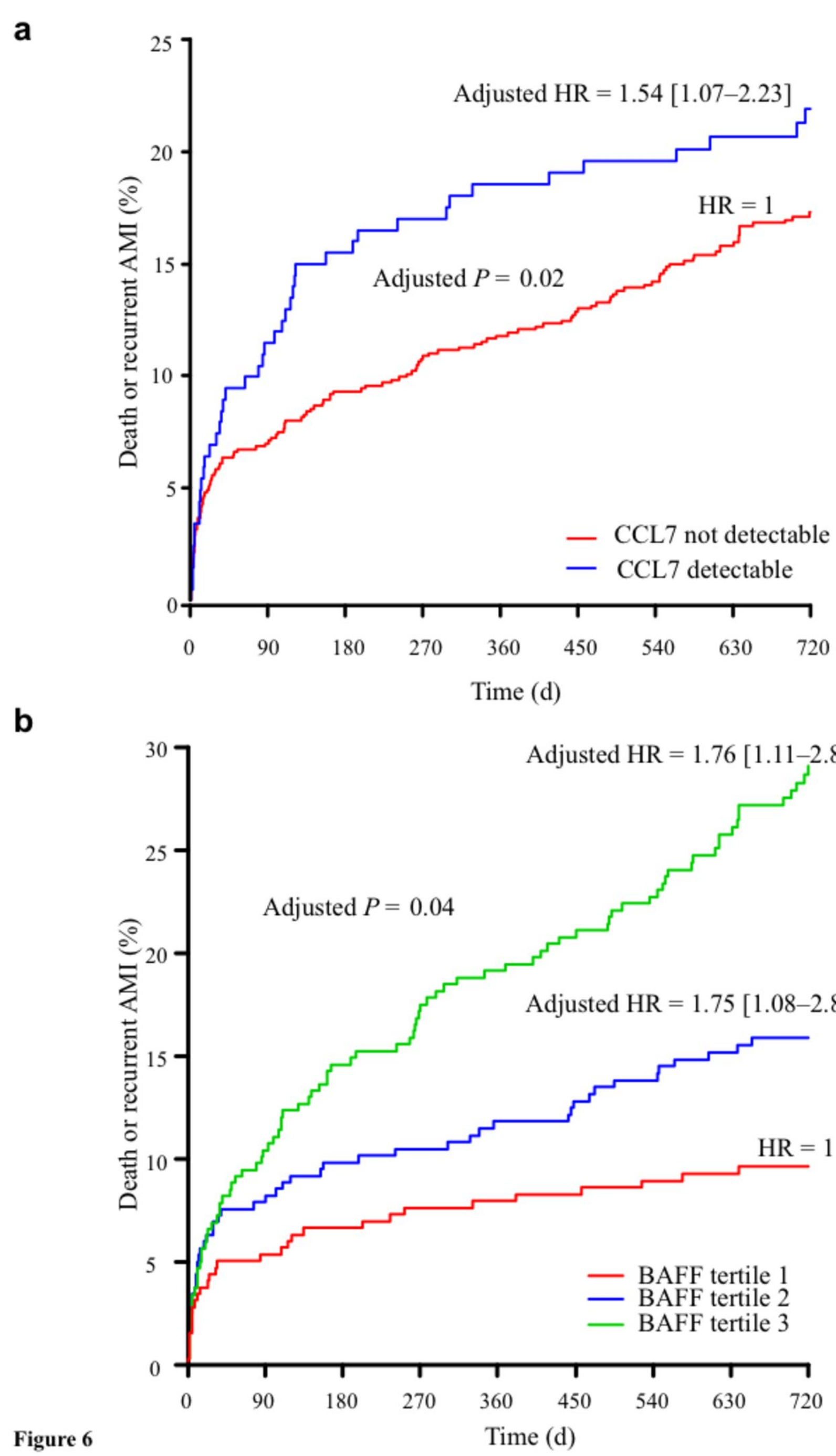
a
Adjusted HR = 1.54 [1.07–2.23]
HR = 1
Adjusted P = 0.02
CCL7 not detectable
CCL7 detectable
Death or recurrent AMI (%)
Time (d)
b
Adjusted HR = 1.76 [1.11–2.82]
Adjusted P = 0.04
Adjusted HR = 1.75 [1.08–2.84]
HR = 1
BAFF tertile 1
BAFF tertile 2
BAFF tertile 3
Death or recurrent AMI (%)
Time (d)

Figure 6